

Rheology and properties of melt-processed poly(ether ether ketone)/multi-wall carbon nanotube composites

D.S. Bangarusamath^{a,*}, Holger Ruckdäschel^b, Volker Altstadt^a, Jan K.W. Sandler^b,
Didier Garray^c, Milo S.P. Shaffer^{d,**}

^a Polymer Engineering, University of Bayreuth, D-95440 Bayreuth, Germany

^b BASF SE, D-67056 Ludwigshafen, Germany

^c SIRRIS, Liege Science Park, 4102 Seraing, Belgium

^d Department of Chemistry, Imperial College, London, SW7 2Az, UK

ARTICLE INFO

Article history:

Received 15 February 2009

Received in revised form

21 September 2009

Accepted 22 September 2009

Available online 26 September 2009

Keywords:

Carbon nanotubes

Poly(ether ether ketone)

Rheology

ABSTRACT

Poly(ether ether ketone) (PEEK)/multi-wall carbon nanotube (MWNT) composites containing up to 17 wt% filler were prepared using a twin screw extruder. Transmission electron microscopy (TEM) images reveal that the MWNTs were homogeneously dispersed in the PEEK matrix. Linear viscoelastic measurements show that both complex viscosity and moduli increase with increasing MWNT concentration. The storage modulus, G' exhibits a dramatic seven order increase in magnitude around 1 wt%, leading to a solid-like low-frequency behaviour at higher loadings; the effect can be attributed to network formation at a rheological percolation threshold. Rheotens measurements show that the melt strength also increases significantly on addition of nanotubes, however, the drawability decreases. An analytical Wagner model was used to calculate the apparent elongational viscosity over a wide range of elongational rates, and to reveal significant increases on addition of MWNTs, with a similar threshold behaviour. The electrical response is also dominated by percolation effects, increasing by nearly 10 orders of magnitude from 10^{-11} to 10^{-1} S/cm, on the addition of only 2 wt% MWNTs. In contrast, the thermal conductivity and tensile elastic modulus of the composites increased linearly with nanotube content, rising by 130% and 50%, at 17 wt% MWNTs, respectively.

© 2009 Elsevier Ltd. All rights reserved.

1. Introduction

Theoretical and experimental studies have shown that perfect, individual carbon nanotubes (CNTs) possess a range of exceptional properties, most notably a tensile strength of up to 50–100 GPa and thermal conductivities higher than diamond [1,2]. The combination of these properties with very low densities, has encouraged studies of CNTs as fillers for high-performance polymer composites. Whilst promising results have been obtained, progress has been limited by the intrinsic quality of CNTs available in bulk quantities, and processing difficulties associated with their dispersion, orientation, and interaction within the matrix. It is important that the CNTs are homogeneously dispersed throughout the matrix without reducing their intrinsic aspect ratio. Thermoplastic melt processing is

a simple, large scale processing technique that is probably the most straightforward route to polymer nanocomposites.

Shear intensive melt mixing, particularly twin screw extrusion, has been used to prepare a wide range of nanotube-polymer blends, including matrices such as polyethylene [3,4], polypropylene [5,6], polystyrene [7], poly(ethylene terephthalate) [8], polycarbonate [9,10], poly(lactic acid) [11] and polyamide [12]. Typically, these blends show improved tensile strength and modulus, but reduced ductility [13,14]. Although electrical percolation can occur at very low loadings in certain nanotube-polymer systems [15], commercial interest has focused on the electrical conductivity obtained at relatively modest loadings of nanotubes. Thermoplastic systems usually electrically percolate at around 1–5 wt%, in line with expectations from excluded volume theory. Essentially, the high aspect ratio of the CNTs allows the statistical formation of a random network at much lower concentrations than for equiaxed fillers. Lower percolation thresholds are associated with kinetically-stabilised networks formed by nanotube agglomeration [16]. Higher thresholds are associated with coating or grafting of the polymer on the CNTs, limiting intertube contacts, or with a high degree of alignment [17].

* Corresponding author. Tel.: +49 921557460; fax: +49 921557473.

** Corresponding author. Tel.: +44 2075945825; fax: +44 2075945801.

E-mail addresses: bangaru.samath@uni-bayreuth.de (D.S. Bangarusamath), m.shaffer@imperial.ac.uk (M.S.P. Shaffer).

The addition of nanotubes can improve polymer properties but is often accompanied by changes in processing characteristics. A number of researchers [5,9,18], have reported a significant increase in viscosity and melt elasticity with increasing nanotube content, particularly at low frequencies. More complex behaviours have been attributed to the selective adsorption of particular molecular weight fractions from the polymer [19]. The general rise in viscosity is expected on adding hard, high aspect ratio particles, which sweep out large hydrodynamic volumes that significantly interact above a critical filler volume fraction. For CNTs, an analogy can be drawn between this rheological percolation and the electrical effects already discussed; the thresholds are often similar but not necessarily identical. For example, Pötschke et al. prepared well-dispersed MWNT-polycarbonate composites which demonstrated electrical and rheological percolation thresholds of 1 wt% and 0.5 wt%, respectively [9,18,20].

Rheological studies of nanocomposite melts are valuable both for improving processing conditions, and for understanding the fundamental characteristics of the nanoscale materials. Percolation effects are sensitive to filler aspect ratio, which itself may be influenced by processing conditions. In CNT composites, the goal is usually to maximize the dispersion whilst minimizing the damage (especially breakage) of the nanotubes; rheological studies should allow this balance to be optimized. Shear flows are most relevant to dispersion and basic blend processing, and have been the focus of existing nanotube studies. On the other hand, elongational flow properties are of great importance for many polymer processes such as foaming, film blowing and fibre spinning which involves extensive stretching of polymer. As yet, only limited data is available on the elongational rheology of CNT and carbon nanofibre (CNF) systems [21,22].

Poly(ether ether ketone) (PEEK) is an high-performance engineering plastic with a high glass transition and melt temperature, excellent mechanical properties, and good solvent and abrasion resistance. In our previous studies, CNF-reinforced PEEK composites were fabricated on a large scale by twin-screw extrusion, showing improved mechanical [23] and tribological properties [24]. The addition of CNFs also improved the elongational flow properties in the PEEK melt [22], stabilizing the production of PEEK/CNF foams. At the same time, the CNF-reinforced cell walls and struts in the final solid foam, improved mechanical and other properties [25]. The goal of the current study was to explore the effect of replacing the CNFs with smaller diameter, higher crystallinity CNTs. The nanotubes are expected to have intrinsically superior properties, and therefore to retain a higher aspect ratio; improvements in both rheological and composite properties might, therefore, be obtained at lower concentrations. In addition, since PEEK is a high cost, high performance polymer, improvements obtained by adding CNTs are relatively likely to be cost-effective. To our knowledge, there is very little published information in the scientific literature on CNT-filled PEEK composites, either on their properties or rheology [26,27]. In this paper, we report the fabrication of PEEK/MWNT nanocomposites using melt blending and systematically investigate, the filler dispersion, morphology and microstructure formation with respect to the rheological (both under shear and elongation), electrical, thermal, and mechanical properties of the composites.

2. Experimental

2.1. Materials

A semi-crystalline poly(ether ether ketone) (PEEK), Victrex PEEK 151 grade with molecular weight of 27 kg/mol was used as the matrix. Multi-wall carbon nanotubes (MWNTs), Nanocyl[®]-7000,

with an average diameter of about 9.5 nm and a length of 1.5 μm , as stated by the manufacturer, were obtained from Nanocyl Co., Belgium. According to the datasheet, these nanotubes are produced via the catalytic carbon vapour deposition (CCVD) process with a carbon purity of 90% and a surface area of 250–300 m^2/g .

2.2. Melt processing and sample preparation

Poly(ether ether ketone)/multi-wall carbon nanotubes composites were prepared by melt-compounding using a twin screw extruder. PEEK containing 2, 5, 10 and 17 wt% of MWNTs were initially prepared using a MAPRE co-rotating twin screw extruder equipped with a gravimetric metering device from Colortronic. The screw had a diameter of 30 mm with $L/D = 33$. Compounding was carried out at a screw speed of 200 rpm with the maximum barrel temperature set at 360 °C and a flow rate of 10 kg/h (for low concentration) and 6.6 kg/h (for 17 wt% MWNT). The master batch containing 17 wt% MWNTs was then further diluted to provide lower concentrations of 0.25, 0.5, 1 and 1.5 wt% nanotubes in PEEK151, using a Berstorff ZE extruder with a screw diameter of 25 mm, $L/D = 33$. Prior to processing, the materials were dried in a vacuum oven at 120 °C for 12 h. The strands leaving the extruder were quenched in a water bath and pelletized. The granulates were subsequently dried at 120 °C under vacuum and then compression molded into disks for dynamic shear rheological measurements. The as-prepared granulates were used for steady shear capillary and Rheotens measurements. The sample nomenclature used for the discussion of the results is reported in Table 1.

2.3. Characterisation

2.3.1. Shear rheological measurements

Both dynamic and steady shear experiments were performed to probe the role of nanotubes on the viscoelasticity of the PEEK matrix. Dynamic shear measurements were performed using an Advanced Rheometric Expansion System (ARES) using parallel plate geometry (25 mm diameter and 1 mm gap). All samples were tested at 360 °C, under nitrogen, after drying at 120 °C in vacuum, in order to prevent oxidation of the specimens. Initially, dynamic strain sweeps were performed to determine the linear viscoelastic regime (LVR), followed by time sweeps at 360 °C to verify the thermal stability of the PEEK samples. Dynamic frequency sweep measurements were then performed in the frequency range from 0.1 to 500 rad/s using a strain amplitude within the linear viscoelastic regime. Dynamic temperature sweep experiments were conducted by varying temperature, starting from 400 °C and cooling down to 310 °C at a rate of 5 °C/min and a frequency of 1 rad/s. Steady shear viscosity experiments at very high shear rates (up to 10^4 s^{-1}) were performed using a Göttfert Rheograph 6000, high-pressure capillary rheometer with die diameter of 1 mm ($L/D = 30$), at 360 °C.

Table 1
Low frequency slope of G' and G'' for neat PEEK and its nanocomposites.

Sample	Nanotube content (wt%)	Low-freq slope of G' vs ω	Low-freq slope of G'' vs ω
PEEK	–	1.81	0.99
PEEK-NT-0.25	0.25 ^a	1.36	0.94
PEEK-NT-0.5	0.5 ^a	1.17	0.94
PEEK-NT-1.0	1.0 ^a	0.51	0.64
PEEK-NT-1.5	1.5 ^a	0.10	0.59
PEEK-NT-2.0	2.0	0.05	0.22
PEEK-NT-5.0	5.0	0.03	0.17
PEEK-NT-10	10	0.02	0.09
PEEK-NT-17	17	0.03	0.05

^a Diluted from PEEK-NT-17 Masterbatch.

2.3.2. Elongational measurements

Uniaxial elongational measurements were performed using a Göttfert Rheotens apparatus and Elongational Viscosity Fixture (EVF) from TA instruments. The melt strength experimental set-up combined a high-pressure capillary rheometer and the Rheotens unit. A high pressure capillary rheometer provided the polymer melt strand at a piston speed of 0.3 mm/s (corresponding to a shear rate of 43.2 s^{-1}) extruded through a capillary die ($L/D = 30/2$) at a barrel temperature of 360 °C. The melt strand was then fed between the copper draw-down wheels placed 96 mm below the die, and the speed of the wheel was then accelerated linearly at 24 mm/s^2 until the strand broke. The maximum draw-down force and the velocity at break are termed as ‘melt strength’ and ‘drawability’, respectively. Each measurement was repeated at least five times, and the data was then fitted using a Levenberg–Marquardt procedure. For this particular set-up, the cooling effect of the extruded strand within the spin-line is small, and the polymer melt is elongated under quasi-isothermal conditions [28]. By applying an analytical Wagner model, the apparent elongational viscosity was calculated from the Rheotens data, by using the parameters obtained during the fitting procedure [29].

The transient elongational viscosity measurements were performed using an elongational viscosity fixture (EVF) attached to an ARES rotational rheometer. The EVF design is based on the original Meissner concept [30], where two cylinders are used to deform the sample; one cylinder rotates about its own axis whilst also moving on a circular orbit around the fixed force measuring cylinder. Homogeneous and stress-free rectangular samples, with dimensions $12 \times 9 \times 1 \text{ mm}$, were compression-molded using a Weber PW10 hot press at 360 °C and 80 kN. The pre-dried sample was placed on to the cylinders, preheated to 380 °C to adhere the sample and then the elongational test was performed at a constant rate of 1 s^{-1} , at 360 °C, under nitrogen.

2.3.3. Morphological investigation

The morphology and state of carbon nanotube dispersion within the PEEK matrix were evaluated using a field-emission scanning electron microscope (FE-SEM) and transmission electron microscope (TEM). SEM micrographs of cryo-fractured, extruded pellets were taken using a Zeiss 1530 microscope. Ultrathin sections of the nanocomposites (thickness of approx. 60 nm) were cut using a Leica Ultracut E microtome equipped with a diamond knife. TEM was carried out using a Zeiss CEM 902 apparatus at an acceleration voltage of 80 kV.

2.3.4. Electrical conductivity measurements

The AC conductivity measurements were performed in the frequency range from 10^{-1} to 10^6 Hz using a Novocontrol Alpha high-resolution impedance analyzer at room temperature (23 °C). Rectangular bars ($10 \times 4.0 \times 1.3 \text{ mm}$) were cut from the compression-moulded specimens. The cross-sectional areas were coated with conductive silver in order to provide good contact to the specimen. The specific conductivity of the nanocomposites as a function of frequency, $\sigma(\omega)$, was calculated from the modulus of the complex admittance, $|Y^*|$ [15]:

$$\sigma(\omega) = |Y^*(\omega)| \left[t/A \right] \quad (1)$$

where t is the thickness and A is the cross-sectional area of the sample.

2.3.5. Thermal conductivity measurements

Thermal conductivity measurements were performed using a hot disk technique. During the measurement, the sensor was

placed between two PEEK sample pieces with flat surfaces. The thermal conductivity for the sample is calculated based on the evolution of temperature with time. The applied output power to the hot disk sensor was 0.025 W and the typical measurement time was 20 s. The radius of the hot disk sensor used in our measurements was 3.189 mm.

2.3.6. Mechanical properties

ISO-3167 (1A) standard tensile bars were manufactured on an Arburg Allrounder 420 injection-moulding machine at a processing temperature of 395 °C. Prior to testing, all the PEEK-based specimens were heat treated, at 150 °C overnight under vacuum, to ensure a similar degree of crystallinity of the polymer matrix. Tensile test were performed at room temperature with an Instron Corporation Universal testing machine – Serie 4500. According to ISO 527 standard, the cross-head speed was set to 1 mm/min and then increased to 25 mm/min until specimen fracture occurred. Tensile data reported were the average of five independent measurements.

3. Results and discussion

3.1. Morphology and dispersion of MWNTs in the polymer matrix

The morphology and dispersion of carbon nanotube filled PEEK composites, prepared by melt processing, were characterized using both scanning electron microscopy (SEM) and transmission electron microscopy (TEM). In SEM, the fracture surfaces are generally homogenous, suggesting a good dispersion of random nanotubes; however, the fibrillation of the polymer makes identification of specific details difficult (Fig. 1) TEM micrographs (Fig. 2a) provide a clearer view, although over a smaller region; the MWNTs appear to be well-dispersed in the PEEK matrix due to the shear forces applied during melt mixing. The high shear mixing can also result in some breakage of the nanotubes; for example, Kharchenko et al. [5] reported that the aspect ratio of MWNTs in a polypropylene matrix was reduced from 1000 to 300–400 after melt processing. The aspect ratio in the current study is hard to determine from the microtomed TEM sections (which intrinsically cut the nanotubes) but will be discussed further below, in the light of the rheology data. At higher magnification (Fig. 2b) the individual MWNTs are recognized as a long hollow fibre with diameter around 10–15 nm. It can also be seen that the nanotubes are curled, rather than straight, a feature that is likely to reduce their reinforcing efficiency [31].

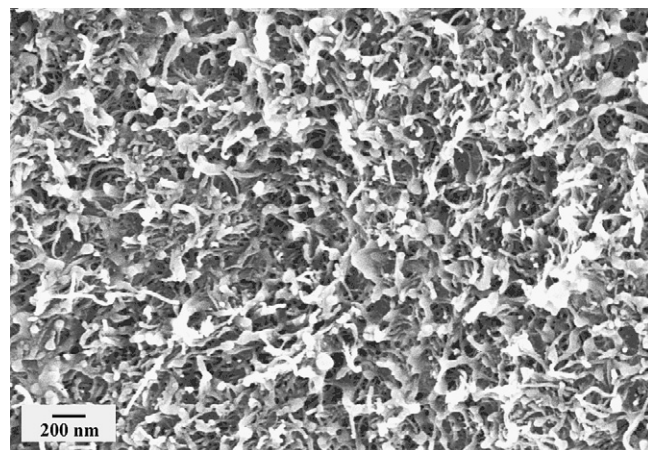


Fig. 1. SEM micrograph of a fracture surface of PEEK containing 17 wt% of MWNT, revealing the dense nanotubes network interpenetrating the polymer matrix.

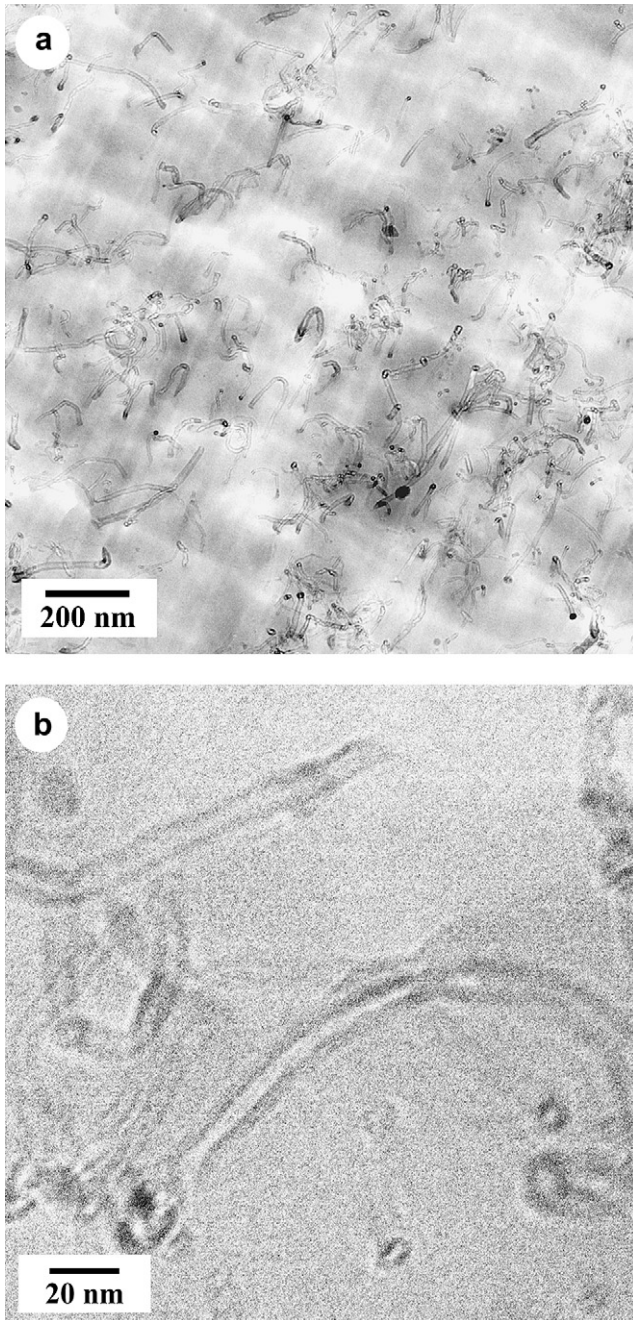


Fig. 2. TEM micrographs of cryo-microtomed PEEK nanocomposite containing (a) 5 wt% MWNTs. (b) Higher magnification showing individual MWNTs.

3.2. Dynamic shear response of PEEK-MWNT composites

Dynamic methods were chosen as they provide detailed information about the elasticity of the sample and the evolution of the microstructure.

3.2.1. Strain dependence of viscoelastic behaviour

Initially, a strain sweep test was applied to the nanocomposite samples in order to determine the linear viscoelastic regime (LVR) and to characterize the strain dependent viscoelastic properties of the samples. Storage modulus, G' , is relatively sensitive to the structural changes within the nanocomposites; as can be seen in Fig. 3, G' exhibits a plateau at low strain amplitudes and a pronounced non-linear region at high strain amplitudes (the so-called Payne effect

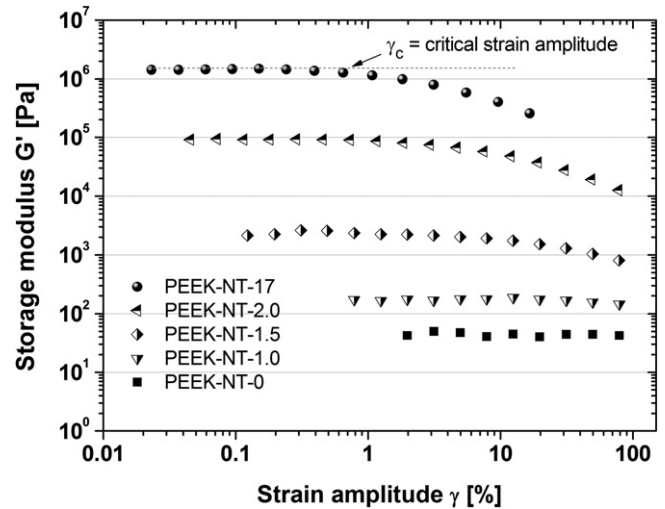


Fig. 3. Strain amplitude dependence of the storage modulus of PEEK and the nanocomposites at 360 °C and frequency of 1 rad/s.

[32]), particularly for the nanocomposite samples. Increasing MWNT content leads to a continuous increase in the magnitude of the plateau modulus and a reduction of the critical strain amplitude, γ_c , (defined as a transition point between linear and non-linear viscoelastic behaviour). For example, the critical strain in the 17 wt% CNT melt ($\sim 0.4\%$) is much lower than that for the 1.5 wt% melt ($\sim 4\%$) or the pure PEEK ($>100\%$). This general behaviour is typical for filler systems in general and CNT-filled systems in particular [32,33]. Some authors have reported that this non-linear behaviour of the composites at high strain amplitudes can be related to the rupture of particle-particle interactions of the physical network [33].

3.2.2. Frequency dependence of viscoelastic behaviour

Dynamic frequency sweep tests were used to explore network formation and microstructure of the nanocomposites, in the LVR. The tests were run at strain amplitude in the range of 0.05–2%. The complex shear viscosity, $|\eta^*|$, generally increases with increasing nanotube content (Fig. 4), by up to six orders of magnitude at low frequencies. At low MWNT concentration (<1 wt%), the blends remain essentially Newtonian, with modest increases of viscosity; however, at higher concentrations, the blends become strongly shear-thinning, whilst retaining a significantly greater viscosity than the pure polymer, even at higher frequencies. In order to understand the processability of these nanocomposites, we have also investigated the steady shear viscosity at high shear rates typical during extrusion and injection moulding processes. Earlier investigations of homogenous melts have shown that the complex viscosity, $|\eta^*|$ (dynamic rotational rheometer), and the steady shear viscosity, η (capillary rheometer), are closely super-imposable for numerically equivalent values of frequency, ω and shear rate, $\dot{\gamma}$ (Cox–Merz rule) [34],

$$|\eta^*(\omega)| = \sqrt{\eta'(\omega)^2 + \eta''(\omega)^2} = \eta(\dot{\gamma}) \quad \text{for } \dot{\gamma} = \omega \quad (2)$$

As can be seen in Fig. 4b, the pure PEEK melt obeys the rule, whereas the filled systems diverge increasingly with higher MWNT content. The lower steady shear viscosity than dynamic complex viscosity may be due to the orientation and interaction of the carbon nanotubes [35]. In dynamic shear tests, the small periodical deformation imposed on the composite melt is too weak to induce significant nanotube orientation. Fibers generally maintain their original randomly oriented state and vibrate at the corresponding frequency

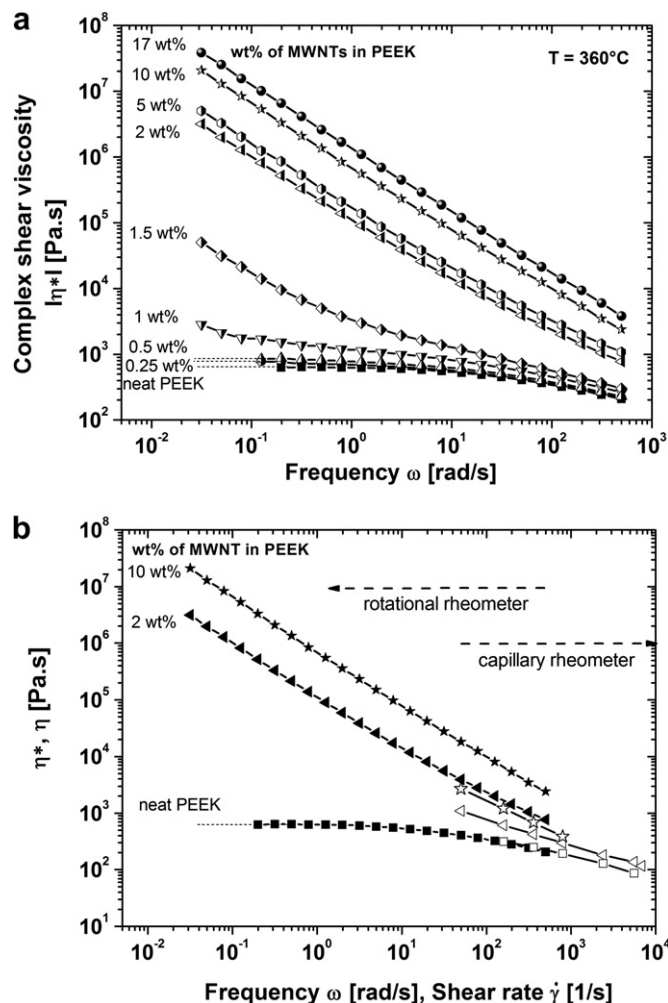


Fig. 4. (a) Complex viscosity of PEEK/MWNT nanocomposites as a function of frequency. (b) Comparison of the complex viscosity (filled symbols) and steady shear viscosity (open symbols) of PEEK and the nanocomposites at 360°C .

in equilibrium positions [36]. Because the viscosity of randomly oriented fiber melt is higher than that of aligned fiber melt for the same fiber aspect ratio and volume fraction, the complex viscosity is larger than the steady shear viscosity measured from capillary tests. Increasing the nanotube content results in a corresponding divergence between the curves of complex viscosity and steady shear viscosity, indicating the contribution of nanotube interactions. This comparison between dynamic and steady shear measurements suggests that the processing behaviour of nanocomposite blends cannot be directly deduced from dynamic tests. The modest magnitude of the increase in steady shear viscosity of the composites as compared to neat PEEK, at high shear rates explains the good processability of the nanocomposite systems. Overall, the viscosity increase due to the CNTs is most pronounced at low frequency and the effect weakens with increasing frequencies due to shear thinning.

Similarly, the additions of MWNTs influence the frequency-dependence of the storage, G' , and loss, G'' , moduli more strongly at low frequencies (Fig. 5). As the nanotube loading increases, the magnitudes of both elastic and loss moduli increase whilst the gradients decrease. According to the theory of linear viscoelasticity [37], the storage and loss moduli of homogeneous polymer systems obey a scaling law behaviour in the low frequency regime, with slopes equal to 2 and unity, respectively; the linear viscoelasticity at low frequencies (terminal zone) reflects fully relaxed polymer

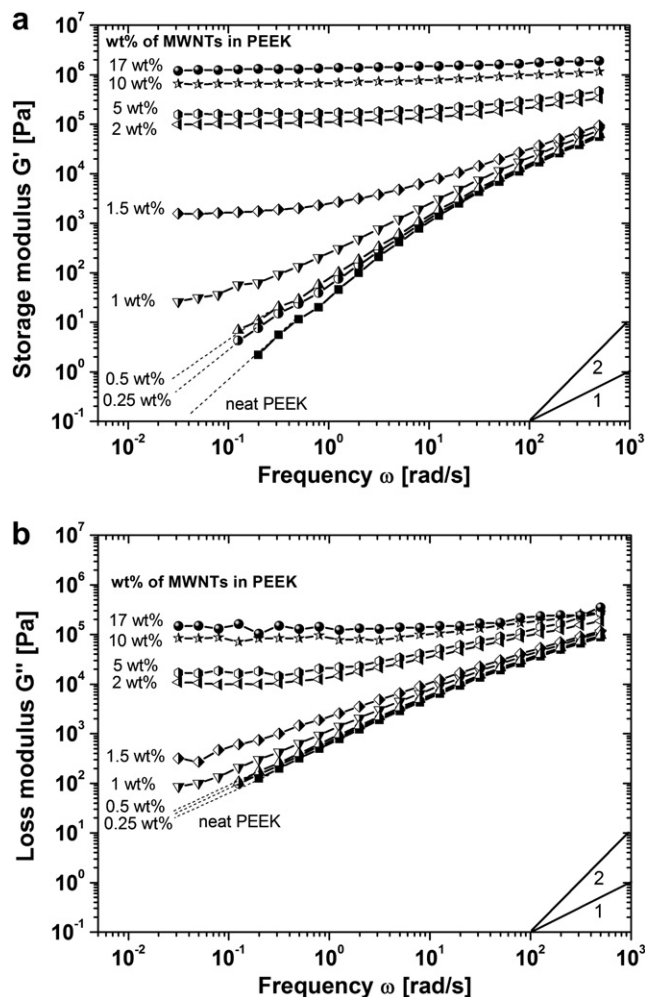


Fig. 5. (a) Storage modulus and (b) loss modulus of PEEK and the nanocomposites as a function of frequency at 360°C .

chains. However, for filled polymer systems, G' and G'' often deviate from this behaviour. As can be seen in Fig. 5 and Table 1, the neat PEEK has a typical terminal regime with the following scaling law: $G' \sim \omega^2$ and $G'' \sim \omega^1$. However, at nanotube loadings above 1 wt%, this terminal behaviour disappears, instead tending to a plateau-like regime (Fig. 5a) that is indicative of a transition from liquid-like to solid-like viscoelastic behaviour. This critical composition (around 1 wt%), correlates with the transitions observed in the other rheological data, and can be identified as a rheological percolation threshold concentration. Similar solid-like behaviours at low frequencies have also been reported in other isotropic particle-filled thermoplastic matrices [5,9,20]. The effect is mainly related to tube-tube interactions and network formation as the interparticle distances decrease, and the hydrodynamic volumes swept out by the particles begin to overlap. Above the critical concentration threshold (1 wt%), tube-tube interactions dominate over polymer-particle interactions, as a filler network becomes established.

Semi-logarithmic plots of phase angle, δ , vs complex modulus, $|G^*|$, also known as van Gurp plots, are useful for exploring the structural differences between the pure matrices and particle-filled systems [3,12]. As shown in Fig. 6, the neat PEEK and the low MWNT concentration curves approach a phase angle of around 90° indicating the viscous flow domination. Above 1 wt% MWNTs, the elastic response is evident in the phase angle that increasingly approaches 0° as the filler loading increases. A good dispersion of

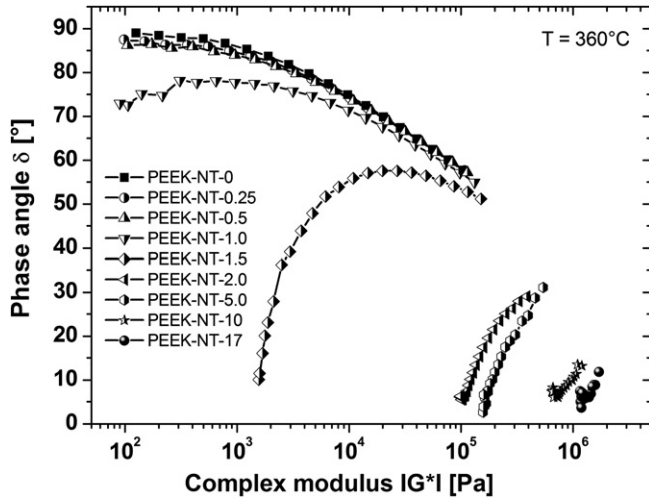


Fig. 6. van Gurp plot for pure PEEK and the nanocomposites at 360 °C.

higher aspect ratio nanotubes could be expected to yield a rheological percolation at lower concentration, and give higher values of the storage modulus.

3.2.3. Temperature dependence of viscoelastic behaviour

The measurements discussed above are all isothermal, whilst real melt processing involves varying temperatures. Indeed, crystallization of semicrystalline polymers and the associated impact on melt rheology are of key importance for controlling the compounding and injection processes. Therefore, the PEEK-MWNT rheology was studied under non-isothermal conditions using dynamic temperature sweeps. As expected, the complex viscosity (Fig. 7) slowly increases on decreasing the temperature until reaching the onset of crystallization (T_c – onset) where the viscosity increases sharply. The addition of MWNTs broadens the transition and slightly increases the onset temperature, though only by about 5 °C, suggesting a nucleation effect; no such effect was observed previously for carbon nanofibres [23], but the surface area of the nanotubes used here is more than an order of magnitude greater. It is important to note that on increasing MWNTs concentration, the sensitivity of the complex viscosity to temperature becomes progressively weaker.

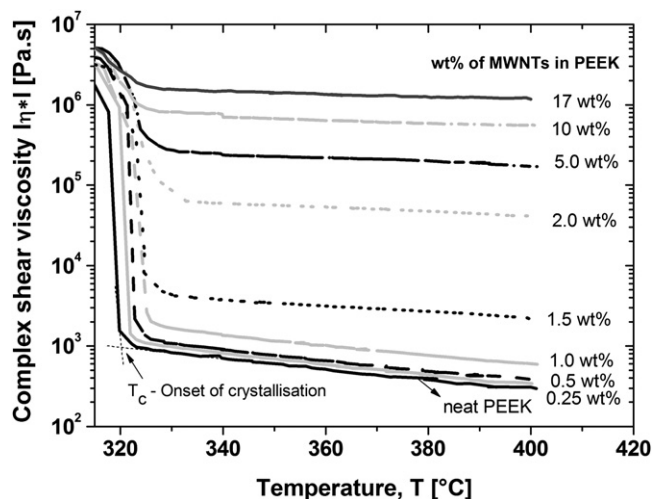


Fig. 7. Complex shear viscosity of PEEK and the nanocomposites as a function of temperature at a cooling rate of 5 °C/min and frequency of 1 rad/s.

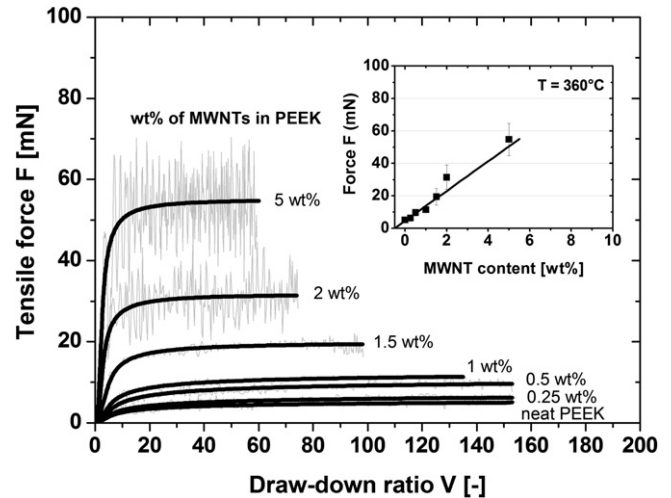


Fig. 8. Experimental average Rheotens curves of PEEK and the nanocomposites at 360 °C.

3.3. Elongational response of PEEK-MWNT composites

3.3.1. Melt strength measurements

Fig. 8 shows the results of the Rheotens experiments, as a plot of tensile force, F vs. draw-down ratio, V (draw-down velocity of the wheel/die exit velocity of the melt, v_r/v_0). As can be seen, the addition of MWNTs substantially increases the melt strength; however, the drawability decreases significantly at higher MWNT content (>1 wt%). At low MWNT concentration (<1 wt%), the drawability appears unaffected; with the melt strand remaining intact up to the maximum set velocity. By adding 5 wt% MWNTs, the melt strength was increased nearly ten-fold, although the drawability more than halved. Above 5 wt% MWNTs, the melt strand broke before a measurement could be obtained. The increase in melt strength can be attributed to the reinforcing effect of the aligned nanotubes on the molten matrix and the stress intensification in the intervening matrix. Above the rheological percolation threshold (around 1 wt%) the ‘entanglement’ of the nanotubes, and the associated elastic character of the system, increases the melt strength dramatically but limits the drawability on the relevant timescale.

3.3.2. Elongational viscosity measurements

Melt strength measurements provide only an indication of the elongation behaviour of polymer melts. In order to understand the complete process, it is important to consider the differential stretching rate of the polymer; specifically, the elongational viscosity, η_E , as can be measured as a function of elongational rate, $\dot{\epsilon}$, using an EVF. At a constant elongational rate, $\dot{\epsilon} = 1 \text{ s}^{-1}$, the elongational viscosity of pure PEEK increases with time, t (Fig. 9). At large times, the elongational viscosity attains a stationary value close to the linear visco-elastic prediction, $3\eta^0(t)$. The nanocomposite blends display a similar behaviour but elongational viscosity increases with increasing filler content. At 5 wt% MWNTs, the elongational viscosity of PEEK is enhanced by nearly an order of magnitude, but strain softening occurs at longer times. Similar increases in elongational viscosity have been reported recently, on addition of MWNTs to polypropylene [38]. It is well documented in literature that increased elongational viscosity can reduce sag and helps to prevent cell coalescence during foaming processing, effectively widening the processing window, especially for the semi-crystalline polymers [25]. Deformation during the foaming process typically occurs over a short period of time, just a few seconds, translating into strain rates of $1\text{--}5 \text{ s}^{-1}$ [39]. However,

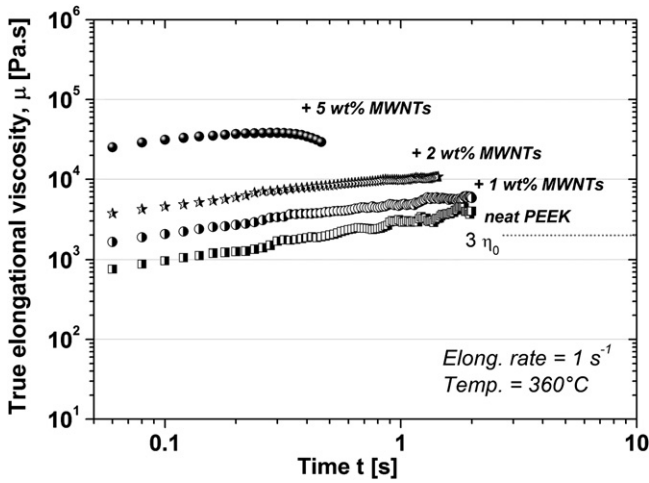


Fig. 9. Transient elongational viscosity as a function of time for PEEK and the nanocomposites, at 360 °C.

during film blowing or fibre spinning processes, the polymer experiences very high strain rates, of up to 100 s⁻¹ [40]. Measurements of elongational viscosity of polymer melt at such high elongational strain rates are difficult to perform due to the instrumental limitations of commercial elongational rheometers.

Laun and Schuch [41] provide an alternative approach; they estimate the elongational viscosity from Rheotens data (tensile force vs. draw-down ratio) and have observed a reasonable agreement with results obtained from elongational experiments performed at constant elongational rates. A direct conversion of the measured Rheotens data into an elongational viscosity is complex, as a non-uniform strain rate is applied along the melt strand. Following a detailed analysis of the complex deformation of the polymer melt strand, an analytical model was proposed by Wagner et al. [29]. Following this approach, the measured force–velocity curve can be fitted using the Levenberg–Marquardt procedure; from the obtained four free fitting parameters, the elongational viscosity can be calculated. More details on the Wagner constitutive equations can be found elsewhere [22,29]. The pure PEEK (Fig. 10) shows an elongational strain hardening behaviour for strain rates up to about 0.5 s⁻¹, where the elongational viscosity reaches a maximum

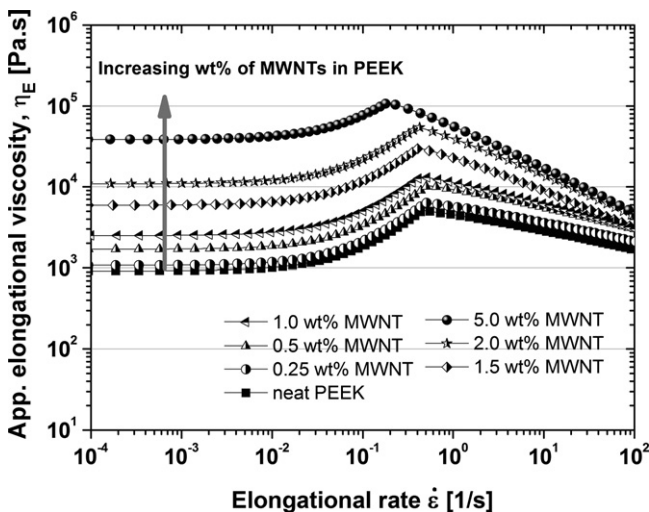


Fig. 10. Apparent elongational viscosity as a function of the elongational rate for PEEK-MWNT composites calculated from the Rheotens curves using Wagner model [29].

before continuously decreasing at higher strain rates (elongational thinning). Addition of MWNTs increases the elongational viscosity significantly at low rates, however, the nanocomposite blends exhibit stronger elongational thinning at higher rates, possibly due to the orientation of the nanotubes. The apparent elongational viscosities calculated using the analytical model are in good agreement with the direct measurements obtained using the EVF (Fig. 9) at $\dot{\epsilon} = 1 \text{ s}^{-1}$. However, the strain hardening behaviour seems to be over-estimated by the model. The elongation thinning behaviour obtained at high elongational rates, is likely to be useful for better understanding of high-speed operation process and for the design and simulation of other industrial processes.

3.4. Electrical conductivity of PEEK/MWNT composites

The conductivity of neat PEEK is less than around 10⁻¹¹ S/cm, as expected for an insulating material (Fig. 11). The addition of up to 1 wt% MWNTs shows no effect on conductivity, however, a sharp increase by at least nine orders of magnitude was observed between 1 and 1.5 wt% MWNTs. The absolute conductivity at 1.5 wt% of MWNTs already satisfies the antistatic criterion (10⁻⁸ S/cm) relevant to a number of applications. Many authors [16], have reported similar electrical percolation effects in composite materials containing a conductive component embedded in an insulating matrix. Clearly, filler network formation affects both rheological and electrical percolation in a related fashion. However, some researchers [18,20] report that the electrical percolation is slightly higher than the rheological percolation due to the different mechanisms associated with interparticle interaction. According to Du et al. [20], the rheological percolation threshold is reached when the distance between two nanotubes becomes smaller than the radius of gyration of the polymer chains, whereas for electrical percolation, the nanotubes must approach sufficiently to allow electron hopping or tunneling. In the current study, the shear and elongation rheological, and electrical percolation thresholds occur at similar loading fractions, although a detailed analysis will be provided elsewhere [42].

3.5. Thermal/mechanical properties of PEEK/MWNT composites

In contrast, the thermal conductivity of PEEK (Fig. 12) increases linearly with MWNT loading fraction, and no percolation effects are observed; the pure PEEK thermal conductivity of 0.3 W/mK

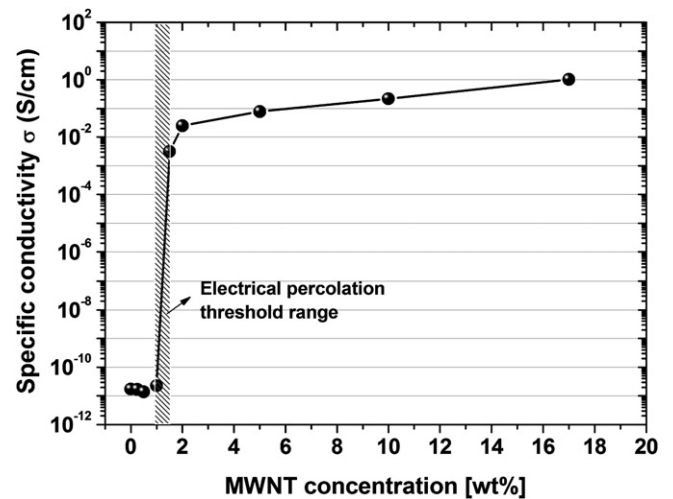


Fig. 11. Semi-log plot of the specific composite conductivity as a function of nanotube concentration at a fixed frequency of 1 Hz.

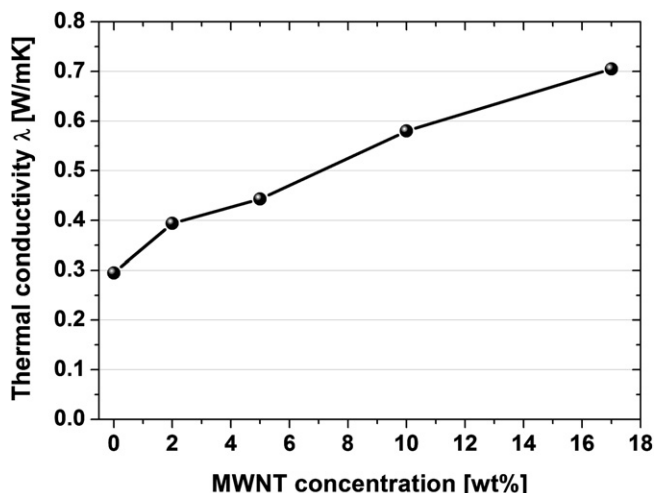


Fig. 12. Thermal conductivity of PEEK nanocomposite as a function of MWNT concentration.

becomes more than doubles to 0.7 W/mK, at 17% MWNT. The lack of percolation effect is expected for thermal conductivity, due to the much smaller intrinsic difference between the filler and matrix property values [43]. Even the ideal axial thermal conductivity of MWNTs (3000 W/mK) [44] is only a factor of 10^4 greater than that of the matrix, whereas a critical ratio of 10^5 has been suggested for the emergence of percolation phenomena [43]. Below this value, rule-of-mixtures approaches are more appropriate. In fact, the thermal conductivity of these CCVD MWNTs is likely to be significantly lower than that proposed for perfect nanotubes. In addition, scattering at the large surface area between the nanotubes and the matrix is thought to account for the relatively limited improvements in thermal conductivity observed in nanotube composites, so far [45].

The tensile modulus of the PEEK nanocomposites (Fig. 13) also increases approximately linearly with nanotube content, mirroring the thermal conductivity data. The rule-of-mixtures increase in stiffness is consistent with previous data on CNF-loaded PEEK [23], and suggests, as expected, an effective modulus for these CCVD MWNTs which is significantly lower than that of idealized nanotubes. A detailed interpretation of the composite stiffness and other mechanical properties, below the crystallization temperature, requires a more detailed study of the influence of the nanofiller on the polymer morphology; changes in matrix crystallinity or

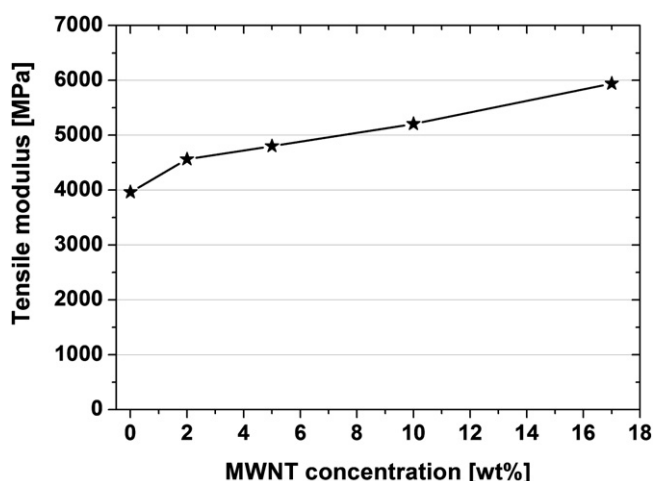


Fig. 13. Tensile modulus of PEEK/MWNT composites.

crystallite size are known to influence the mechanical performance [46], the nucleation effects suggested by the temperature sweep rheological data (Fig. 7) are to be expected.

4. Conclusion

Homogenous multi-wall carbon nanotube/poly(ether ether ketone) composites have been fabricated using a twin-screw extruder. The rheological properties of these nanocomposites PEEK blends were investigated under both shear and elongational flows. Our small-amplitude dynamic shear rheological studies showed that both the complex viscosity, $|\eta^*|$ and moduli (G' and G'') increase monotonically with increasing MWNT content. For composites containing more than 1 wt% MWNTs content, a strong shear thinning behaviour was observed with a plateau which appears in the storage modulus, G' , at low frequencies, indicating the formation of a percolated nanotube network that responds elastically over long timescales. Rheotens measurements show that the tensile force (melt strength) increases dramatically with the nanotube loading, while the draw-down ratio (drawability) significantly decreases. Transient melt elongational measurements, at a fixed elongational rate (1 s^{-1}), confirm that the elongational viscosity of PEEK significantly increases on addition of MWNTs. The elongational viscosity estimated from the Rheotens data, provides information over a range of elongation rates, with similar increases in viscosity at low rates and thinning at high rates. In-situ scattering studies of the blends under different flow fields may provide useful information about the relative degree of polymer and nanotube alignment, in the future.

The electrical conductivity of the PEEK/MWNT composites displayed a similar percolation behaviour to the rheological data. In contrast, both the tensile stiffness and thermal conductivity data increased only linearly with MWNT loading fraction, but, nevertheless, demonstrated significant improvements. The addition of MWNTs to PEEK improves the mechanical, thermal, and wear properties of an already high performance matrix, without harming important characteristics, such as thermal and chemical resistance. In addition, the presence of nanotubes may actually improve the ease of processing these nanocomposites, particularly in applications such as foaming. The rheological data presented above will aid the understanding and development of the thermoplastic processing of such systems, and may be extended to other thermoplastic matrices.

Acknowledgments

Financial support by the Bayerische Forschungsstiftung (BFS), Germany, through grant 'CELLJECT200X' and from the EU FP6 project 'CANAPE' is greatly acknowledged. The authors would like to thank Prof. Moos, Department of Functional materials, University of Bayreuth for use of their electrical conductivity equipment.

References

- [1] Advani SG. Processing and properties of nanocomposites. World Scientific Publishing Co.; 2007.
- [2] Coleman JN, Khan U, Blau WJ, Gun'ko YK. Carbon 2006;44:1624–52.
- [3] McNally T, Pötschke P, Halley P, Murphy M, Martin D, Bell SEJ, et al. Polymer 2005;46:8222–32.
- [4] Tang W, Santare MH, Advani SG. Carbon 2003;41:2779–85.
- [5] Kharchenko SB, Douglas JF, Obrzut J, Grulke EA, Migler KB. Nature Materials 2004;3:564–8.
- [6] Lee SH, Eunnari CHO, Jeon SH, Youn JR. Carbon 2007;45:2810–22.
- [7] Choi YJ, Hwang SH, Hong YS, Kim JY, Ok CY, Huh W, et al. Polymer Bulletin 2005;53:393–400.
- [8] Li Z, Luo G, Wei F, Huang Y. Composites Science and Technology 2006;66:1022–9.

- [9] Pötschke P, Abdel-Goad M, Alig I, Dudkin S, Lellinger D. *Polymer* 2004;45: 8863–70.
- [10] Lin B, Sundararaj U, Pötschke P. *Macromolecular Materials and Engineering* 2006;291:227–38.
- [11] Villmow T, Pötschke P, Pegel S, Häussler L, Kretzschmar B. *Polymer* 2008;49: 3500–9.
- [12] Meincke O, Kaempfer D, Weickmann H, Friedrich C, Vathauer M, Warth H. *Polymer* 2004;45:739–48.
- [13] Harris PJF. *International Materials Reviews* 2004;49:31–43.
- [14] Andrews R, Weisenberger MC. *Current Opinion in Solid State and Materials Science* 2004;8:31–7.
- [15] Sandler JKW, Kirk JE, Kinloch IA, Shaffer MSP, Windle AH. *Polymer* 2003; 44:5893–9.
- [16] Bauhofer W, Kovacs JZ. *Composite science and technology*, in press.
- [17] Shaffer MSP, Windle AH. *Advanced Materials* 1999;11:937–41.
- [18] Hu G, Zhao C, Zhang S, Yang M, Wang Z. *Polymer* 2006;47:480–8.
- [19] Zhang Q, Lippits DR, Rastogi S. *Macromolecules* 2006;39:658–66.
- [20] Du F, Scogna RC, Zhou W, Brand S, Fischer JE, Winey KI. *Macromolecules* 2004;37:9048–55.
- [21] Handge UA, Pötschke P. *Rheologica Acta* 2007;46:889–98.
- [22] Bangarusam path DS, Ruckdäschel H, Altstädt V, Sandler JKW, Wassner E, Shaffer MSP. *Polymer engineering and science*, submitted.
- [23] Sandler J, Werner P, Shaffer MSP, Demchuk V, Altstädt V, Windle AH. *Composite Part A* 2002;33:1033–9.
- [24] Werner P, Altstädt V, Jaskulka R, Jacobs O, Sandler JKW, Shaffer MSP, et al. *Wear* 2004;257(9):1006–14.
- [25] Werner P, Verdejo R, Wöllecke F, Altstädt V, Sandler JKW, Shaffer MSP. *Advanced Materials* 2005;17:2864–9.
- [26] Deng F, Ogasawara T, Takeda N. *Composites Science and Technology* 2007;67:2959–64.
- [27] Diez-Pascual AM, Naffakh M, Gomez MA, Marco C, Ellis G, Martinez MT, Anson A, Gonzalez-Dominguez JM, Martinez-Rubi Y, Simard B. *Carbon* 2009; 47:3079–90.
- [28] Muke S, Ivanov I, Kao N, Bhattacharya SN. *Journal of Non-Newtonian Fluid Mechanics* 2001;101:77–93.
- [29] Wagner MH, Bernnat A, Schulze V. *Journal of Rheology* 1998;42:917–28.
- [30] Meissner J, Hostettler J. *Rheologica Acta* 1994;33:1–21.
- [31] Fischer FT, Bradshaw RD, Brinson LC. *Applied Physics Letters* 2002;80:4647–9.
- [32] Payne AR. *Journal of Applied Polymer Science* 1962;19:57–63.
- [33] Bokobza L. *Polymer* 2007;48:4907–20.
- [34] Cox WP, Merz EH. *Journal of Polymer Science* 1958;118:619–22.
- [35] Kinloch IA, Roberts SA, Windle AH. *Polymer* 2002;43:7483–91.
- [36] Guo R, Azaiez J, Bellehumeur C. *Polymer Engineering and Science* 2005;45:385–99.
- [37] Ferry JD. *Viscoelastic properties of polymers*. 3rd ed. New York: John Wiley & Sons; 1980.
- [38] Pötschke P, Krause B, Stange J, Münstedt H. *Macromolecular Symposium* 2007;254:400–8.
- [39] Spital P, Macosko CW. *Polymer Engineering and Science* 2004;44:2090–100.
- [40] Collier J, Petrovan S, Patil P, Collier B. *Journal of Materials Science* 2005;40: 5133–7.
- [41] Laun HM, Schuch H. *Journal of Rheology* 1989;33:119–75.
- [42] Bangarusam path DS, Ruckdäschel H, Altstädt V, Sandler JKW, Garray D, Shaffer MSP. *Chemical Physics Letter*, in Press.
- [43] Mamunya YP, Davydenko VV, Pissis P, Lebedev EV. *European Polymer Journal* 2002;38:1887–97.
- [44] Kim P, Shi L, Majumdar A, McEuen PL. *Physical Review Letters* 2001;21: 2155021–4.
- [45] Nan CW, Liu G, Lin Y, Li M. *Applied Physics Letters* 2004;85:3549–51.
- [46] Sandler J, Windle AH, Werner P, Altstädt V, Es MV, Shaffer MSP. *Journal of Materials Science* 2003;38:2135–41.